

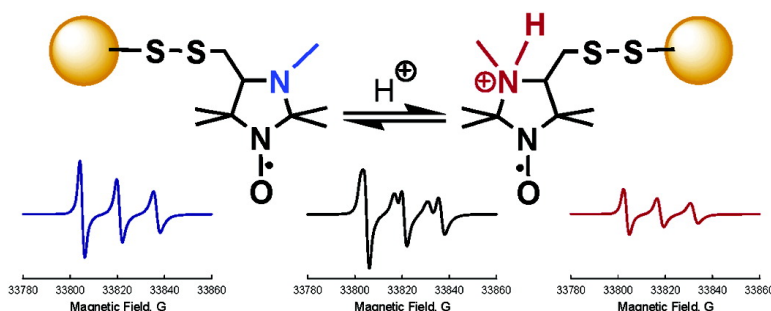
Communication

Site-Directed Electrostatic Measurements with a Thiol-Specific pH-Sensitive Nitroxide: Differentiating Local pK and Polarity Effects by High-Field EPR

Alex I. Smirnov, Andres Ruuge, Vladimir A. Reznikov, Maxim A. Voinov, and Igor A. Grigor'ev

J. Am. Chem. Soc., **2004**, 126 (29), 8872-8873 • DOI: 10.1021/ja048801f • Publication Date (Web): 30 June 2004

Downloaded from <http://pubs.acs.org> on March 31, 2009



More About This Article

Additional resources and features associated with this article are available within the HTML version:

- Supporting Information
- Links to the 3 articles that cite this article, as of the time of this article download
- Access to high resolution figures
- Links to articles and content related to this article
- Copyright permission to reproduce figures and/or text from this article

[View the Full Text HTML](#)



ACS Publications
 High quality. High impact.

Site-Directed Electrostatic Measurements with a Thiol-Specific pH-Sensitive Nitroxide: Differentiating Local pK_a and Polarity Effects by High-Field EPR

Alex I. Smirnov,^{*,†} Andres Ruuge,[†] Vladimir A. Reznikov,[‡] Maxim A. Voinov,^{†,‡} and Igor A. Grigor'ev[‡]

Department of Chemistry, North Carolina State University, 2620 Yarbrough Drive, Raleigh, North Carolina 27695-8204, and Novosibirsk Institute of Organic Chemistry, Akad. Lavrent'ev Ave. 9, Novosibirsk 630090, Russia

Received March 2, 2004; E-mail: alex_smirnov@ncsu.edu

Electrostatic interactions and hydrogen bonding play fundamental roles in virtually all aspects of protein structure and function. Solvent polarity and the presence of localized charges affect protein stability. Some biochemical reactions, such as self-cleavage of viral ribozymes, are proposed to occur at the active site through a general acid mechanism and are affected by pK_a values of the side chains involved.¹ In addition, specific protein conformations including refolding on membrane interfaces and insertion into phospholipid bilayers could be triggered by pH.²

While in some cases local electrostatics and residue-specific pK_a values of proteins could be assessed by steady-state and time-resolved fluorescence³ or high-resolution NMR,⁴ these methods have several shortcomings especially when applied to membrane proteins. For example, labeling with fluorescence pH indicators could affect the fine balance of molecular interactions of proteins with the bilayer, while NMR spectra of large proteins are often resolution limited.

Local electric fields and hydrogen bonding can also be observed from changes in nitroxide EPR spectra.^{5,6} In application to proteins the EPR method is based on site-specific incorporation of a nitroxide side chain which reports on local structure and dynamics since its EPR spectrum is sensitive to local protein motion and spin-spin interactions. The chain has a relatively small molecular volume comparable to that of phenylalanine⁷ and, as such, represents minimal perturbation to the protein structure.⁸ To date, almost all site-directed spin-labeling (SDSL) EPR studies have been carried out with methanethiosulfonic acid *S*-(1-oxy-2,2,5,5-tetramethyl-2,5-dihydro-1*H*-pyrrol-3-ylmethyl) ester (MTSL) which has methanethiosulfonate (MTS) thiol-specific attachment group. While MTSL has been proven to be a very useful probe, it cannot be used for local pH determination because its pK_a lies outside the useful range.

Here we describe a more general approach to mapping local pK_a values of peptides with high-field EPR using MTS derivatives of imidazolidine nitroxides. Imidazoline—as well as imidazolidine nitroxides containing a basic function in the heterocycle—are considered to be the most suitable for biophysical applications because of tunable pK_a range, reversible pH effects, and high sensitivity of the EPR spectrum to pH changes.^{9–12} While the use of imidazolidine nitroxides in studies of surface potentials and polarity of phospholipid bilayers and human serum albumin has been described in the past,^{12,13} the covalent attachment employed in those studies was not fully specific. Moreover, previous studies of local pK_a by EPR were based solely on measurements of isotropic nitrogen hyperfine constant A_{iso} , which could be affected by experimental conditions other than proton exchange reactions. One such factor is the solvent polarity. Here we report on differentiating polarity and proton exchange effects by using A_{iso} versus g_{iso} correlation

plots obtained from high-field (HF) EPR at 95 GHz (W-band), thus eliminating the need for additional control EPR experiments.

High specificity of covalent attachment of a pH-sensitive imidazolidine nitroxide to thiols was achieved by synthesizing the MTS derivative, IMTSL, methanethiosulfonic acid *S*-(1-oxy-2,2,3,5,5-pentamethyl-imidazolidin-4-ylmethyl) ester. Scheme 1 and the Supporting Information describe the synthesis.

To calibrate g_{iso} and A_{iso} of IMTSL for pH dependence a series of room-temperature W-band EPR spectra of aqueous solutions of the free label and the label attached to a cysteine (IMTSL-cys) and glutathione (IMTSL-glu) were measured as a function of pH. At intermediate pH the W-band EPR spectra of these compounds consisted of two partially resolved nitroxide components (not shown) characteristic of slow exchange conditions. The spectra were simulated with least-squares program described earlier.¹⁴ The A_{iso} titration data and corresponding least-squares Henderson–Hasselbalch titration curves are shown in Figure 1.

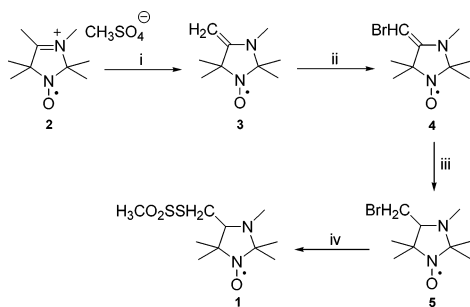
The EPR titration curves in Figure 1 show that for all compounds studied A_{iso} undergoes large (>1.3 G) changes upon protonation of the tertiary amine nitrogen N3. Also, the pK_a 's of IMTSL-cys and IMTSL-glu were respectively shifted to more basic $pK_a = 3.21 \pm 0.04$ and 3.15 ± 0.03 from that of the free label (1.58 ± 0.03 units) while $A_{iso}(\text{base})$ and $A_{iso}(\text{acid})$ were not affected. It is likely that after the labeling the electronegativity of the side chain is reduced. Since the side chain is closer to N3 than to the nitroxide moiety, this decrease in the electronegativity shifts the N3 pK_a to more basic values without any measurable effects on the unpaired electron spin density. Thus, for these small spin-labeled peptides that are not expected to acquire any globular structure it was observed that the presence of other ionizable groups in the side chain have no effects on the IMTSL EPR spectra, which showed only one transition caused by proton exchange reaction at the N3 position.

To elucidate solvent effects on IMTSL W-band EPR spectra, a series of measurements in protic and aprotic solvents were carried out. The data, summarized in Figure 2 as g_{iso} versus A_{iso} plots, suggest a linear correlation. Although previously two different (linear) correlations g_{iso} versus A_{iso} were reported for protic and aprotic solutions of di-*tert*-butyl nitroxide,¹⁵ recent W-band data for 2,2,6,6-tetramethylpiperidin-1-oxy suggested the same g_{iso} versus A_{iso} linear correlation regardless the type of the solvent.¹⁶

One interesting question is whether g_{iso} and A_{iso} for titration curves would fall on the same correlation plot. Figure 2 shows that at pH values below the N3 pK_a the magnetic parameters g_{iso} and A_{iso} clearly fall below the correlation line. We speculate that this deviation is related to the effect of an asymmetric charge located chiefly on N3 onto the oxygen lone-pair orbital of the reporter nitroxide moiety. As one would expect, an acidic form of IMTSL would have a somewhat different charge configuration of the nitroxide moiety that cannot be mimicked by a symmetric rearrangement of the solvent molecules with respect to the axis of the

[†] North Carolina State University.

[‡] Novosibirsk Institute of Organic Chemistry.

Scheme 1^a

^a Reagents and conditions: i, NaHCO₃, H₂O/CHCl₃; ii, dioxane dibromide, Et₃N, 0 °C.; iii, NaBH₄, CH₃OH, 0 °C.; iv, NaSSO₂CH₃, DMSO

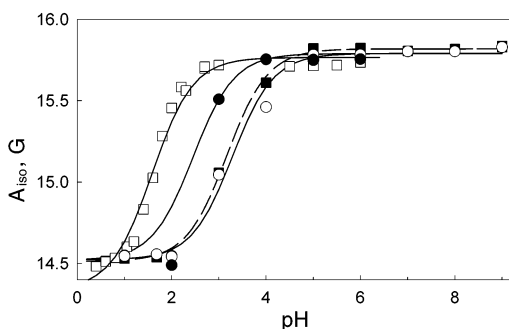


Figure 1. Weighted A_{150} for two-component W-band (95 GHz) EPR spectra as a function of pH and corresponding Henderson–Hasselbalch titration curves (shown as lines): (□) IMTSL; (■) IMTSL–glutathione; (●) IMTSL–P11 (all titration curves – solid lines); (○) IMTSL–cysteine (titration curve – dashed line).

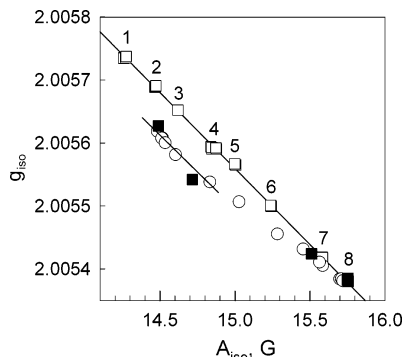


Figure 2. Isotropic magnetic parameters g_{150} and A_{150} from solution W-band EPR spectra. (□) Basic form of IMTSL in 1 (toluene); 2 (acetonitrile); 3 (acetone); 4 (2-propanol); 5 (ethanol); 6 (water/ethanol, 3:7, v/v); and 7 (water/ethanol, 7:3, v/v); 8 (water buffered to pH 6.0). Titration parameters for: IMTSL (○) and IMTSL–P11 (■).

N–O bond occurring in solvents with different polarity. This would result in different correlations between g_{150} and A_{150} that we observed for acidic and basic forms of IMTSL. This difference could be very useful for determining whether the changes in EPR spectra are caused by N3 protonation or by local polarity effects. It is worthwhile to note here that the accurate g factors provided by HF EPR are essential for an unambiguous assignment.

To illustrate utility of IMTSL and HF EPR in site-directed pK_a measurements, we have selectively labeled the thiol group of a synthetic P11 peptide fragment of the laminin B1 chain (Cys–Asp–Pro–Gly–Tyr–Ile–Gly–Ser–Arg). Previous studies have shown that this laminin fragment could inhibit lung tumor colony formation by blocking tumor cell invasion through basement membranes.¹⁷ W-band titration experiments with IMTSL–P11 have shown that upon a decrease in pH the EPR signal splits into two components, similar to that observed for IMTSL–cys and IMTSL–glu. From pH = 6.0 to pH = 3.0 the effective A_{150} decreased only slightly, but at

pH = 2.0 A_{150} was essentially equal to the $A_{150}(\text{acid})$ value for IMTSL (Figure 1). Because at acidic pH one could expect a change in the peptide conformation, only the data from pH = 3 to pH = 6 were fitted to the Henderson–Hasselbalch equation (Figure 1, solid line). Figure 1 demonstrates that for IMTSL–P11 $pK_a = 2.5 \pm 0.1$ is less than that of either IMTSL–glu or IMTSL–cys ($pK_a \approx 3.18$).

It seems possible that local polarity effects arising from the peptide backbone could also explain the A_{150} value observed in our experiments. For example, if the nitroxide ring aligns with a tyrosine, this would decrease the nitroxide local polarity and cause A_{150} to decrease. To rule out this possibility, we have analyzed the correlation plot. Figure 2 shows that g_{150} versus A_{150} plot of the magnetic parameters for IMTSL–P11 (filled squares) closely follows the IMTSL titration curve that falls below the polarity calibration line. Thus, we conclude that the observed changes g_{150} and A_{150} are related to a proton exchange reaction of the nitroxide label but not the local polarity changes.

While small spin-labeled peptides such as, e.g., IMTSL–glu, are expected to be unfolded, a larger P11 peptide could adopt a folded or a partially folded state through tertiary interactions. Specifically for P11, an energy-optimized structure (not shown) places the nitroxide ring in a close proximity to the carboxylic group of the aspartic acid. Because the pK_a of that group of peptides ranges from 2.0 to 4.93 units,^{18,19} it is feasible that the observed shift of the IMTSL–P11 titration curve from that of IMTSL–glu reflects the close proximity of the carboxylic group.

Acknowledgment. Support from NATO LST.CLG.977528 (to A.I.S. and I.A.G.), the Russian Foundation for Basic Research Grant 01-03-32452a (to I.A.G.), the DOE Contract W-31-109-Eng-38 (to A.I.S.), and the ACS PRF (to A.I.S.) is gratefully acknowledged. M.A.V. is thankful to the NSF NATO fellowship for support.

Supporting Information Available: Experimental procedures. This material is available free of charge via the Internet at <http://pubs.acs.org>.

References

- Luptak, A.; Ferre-DrAmare, A. R.; Zhou, K.; Zilm, K. W.; Doudna, J. A. *J. Am. Chem. Soc.* **2001**, *123*, 8447–8452.
- Zhan, H.; Choe, S.; Huynh, P. D.; Finkelstein, A.; Eisenberg, D.; Collier, R. J. *Biochemistry* **1994**, *33*, 11254–11263.
- Cohen, B. E.; McAnaney, T. B.; Park, E. S.; Jan, Y. N.; Boxer, S. G.; Jan, L. Y. *Science* **2002**, *296*, 1700–1703.
- Tollinger, M.; Forman-Kay, J. D.; Kay, L. E. *J. Am. Chem. Soc.* **2002**, *124*, 5714–5717.
- Gullá, A. F.; Budil, D. E. *J. Phys. Chem. B* **2001**, *105*, 8056–8063.
- Steinhoff, H.-J.; Savitsky, A.; Wegener, C.; Pfeiffer, M.; Plato, M.; Möbius, K. *Biochim. Biophys. Acta* **2000**, *1457*, 253–262.
- Feix, J. B.; Klug, C. S. In *Biological Magnetic Resonance*; Berliner, L. J., Ed.; Plenum Press: New York, 1998; Vol. 14, pp 251–282.
- Mchaourab, H. S.; Lietsow, M. A.; Hideg, K.; Hubbell, W. L. *Biochemistry* **1996**, *35*, 7692–7704.
- Khrantsov, V. V.; Volodarsky, L. B. In *Biological Magnetic Resonance*; Berliner, L. J., Ed.; Plenum Press: New York, 1998; Vol. 14, pp 109–180.
- Khrantsov, V. V.; Weiner, L. M.; Grigoriev, I. A.; Volodarsky, L. B. *Phys. Chem. Lett.* **1982**, *91*, 69–72.
- Keana, J. F. W.; Acarregui, M. J.; Boyle, S. L. M. *J. Am. Chem. Soc.* **1982**, *104*, 827–830.
- Khrantsov, V. V.; Weiner, L. M.; Eremenko, S. I.; Belchenko, O. I.; Schastnev, P. V.; Grigor'ev, A. I.; Reznikov, V. A. *J. Magn. Reson.* **1985**, *61*, 397–408.
- Khrantsov, V. V.; Marsh, D.; Weiner, L.; Reznikov, V. A. *Biochim. Biophys. Acta* **1992**, *1104*, 317–324.
- Smirnov, A. I.; Smirnova, T. I. In *Biological Magnetic Resonance*; Berliner, L. J., Bender, C., Eds.; Kluwer: New York, 2004; Vol. 21, pp 277–348.
- Kawamura, T.; Matsunami, S.; Yonezawa, T. *Bull. Chem. Soc. Jpn.* **1967**, *40*, 1111–1115.
- Smirnov, A. I.; Smirnova, T. I. *Appl. Magn. Reson.* **2001**, *21*, 453–467.
- Iwamoto, Y.; Robey, F. A.; Graf, J.; Sasaki, M.; Kleinman, H. K.; Yamada, Y.; Martin, G. R. *Science* **1987**, *238*, 1132–1134.
- Noble, M. A.; Gul, S.; Verma, C. S.; Brocklehurst, K. *Biochem. J.* **2000**, *351*, 723–733.
- Lohse, D. L.; Denu, J. M.; Santoro, N.; Dixon, J. E. *Biochemistry* **1997**, *36*, 4568–4575.

JA048801F